Features of the pulsed cathodoluminescence kinetics of neodymium ion in yttrium-aluminum garnet and yttria

© V.I. Solomonov [1,2], A.V. Spirina [1], A.S. Makarova [1]

[1] Institute of Electrophysics, Ural Branch, Russian Academy of Sciences,
Yekaterinburg, Russia
[2] Ural Federal University after the first President of Russia B.N. Yeltsin,
Yekaterinburg, Russia

E-mail: anniebubnova@mail.ru

The kinetics of pulsed cathodoluminescence of Nd^{3+} ions in single crystals, ceramics, and nanopowders of $Nd^{3+}:Y_3Al_5O_{12}$ ($Nd^{3+}:YAG$) and $Nd^{3+}:Y_2O_3$ under excitation by a 2 ns electron beam with average electron energies of 130, 150, and 170 keV was studied. In this case, the luminescence of these substances occurs after the termination of the electron beam. In $Nd^{3+}:YAG$, there are optical transitions from the $^2F2_{5/2}$ level of the neodymium ion in the ultraviolet and visible regions of the spectrum, as well as from the $^4F_{3/2}$ level in the near infrared region. In $Nd^{3+}:Y_2O_3$, there are not transitions from the $^2F2_{5/2}$ level of the neodymium ion, but infrared luminescence occurs from the $^4F_{5/2}$ and $^4F_{3/2}$ levels. The luminescence kinetics is characterized by rise and decay and it is described by the difference of two exponential functions. It is found that the characteristic luminescence decay times are the lifetimes of the $^2F2_{5/2}$, $^4F_{5/2}$ and $^4F_{3/2}$ emissive levels, and the rise time is determined by their pumping in recombination and relaxation processes. The rise mechanisms of pulsed cathodoluminescence are substantially different from the mechanisms of „phosphor ignition", which occur during ionization and excitation of the phosphor by an external source.

Keywords: pulsed cathodoluminescence, neodymium ion, yttrium-aluminum garnet, yttria, kinetics, rise time, decay time.

1. Introduction

The Nd^{3+} ion is used as an activator in monocrystalline and ceramic active elements $Nd^{3+}:Y_3Al_5O_{12}$ ($Nd^{3+}:YAG$) and $Nd^{3+}:Y_2O_3$ of highly efficient and powerful lasers [1–4]. These materials are interesting in terms of the luminescence study, since the Nd^{3+} ion in them can have two electronic configurations $4f^3$ and $4f^25d^1$ active in luminescence [5,6]. There are many papers relating the study of the Nd^{3+} ions luminescence in these crystal matrices, including the study of the luminescence kinetics [5–9]. Moreover, in most works, the stage of luminescence decay is studied without considering the processes of additional population of emissive levels, which can lead to an erroneous interpretation of the measurement results. This paper presents the results of studying pulsed cathodoluminescence (PCL) of neodymium ions in single crystals and ceramics of yttrium-aluminum garnet, as well as in ceramic and nanopowder samples of yttrium oxide in a wide optical range in order to determine the specific nature of the kinetics of pulsed cathodoluminescence bands, including processes of both rise, and decay.

2. Research methods and objects

The objects of study were laser single crystals and ceramic samples $Nd^{3+}:YAG$ with a neodymium content of 0.85 at.% and about 1 at.%, respectively, as well as ceramic samples and nanopowders of $Nd^{3+}:Y_2O_3$ cubic structure with neodymium content of about 1 at.%. The single crystals were grown at POLYUS Scientific Research Institute (Moscow) by horizontal directional crystallization, ceramics and nanopowders were manufactured at IEP UB RAS according to the method described in [4].

Pulsed cathodoluminescence was excited by an electron beam with duration $t_e = 2$ ns with average energy $E_e = 130$, 150 and 170 keV at current densities $j_e = 85$, 100 and 115 A/cm^2, respectively. The luminescence flux from the sample was taken out by means of a multicore fiber optic waveguide and directed through a collimator to MDR-41 monochromator. The optical radiation receivers were FEU-62 and FEU-100 photomultipliers. The signal from the photomultiplier was recorded with a Keysight DSOX2014A oscilloscope. Irradiation by electrons was carried out in air at room temperature of the samples. The survey luminescence spectrum in the range $200-1200$ nm was recorded using the same equipment. The error of wavelength measurement was 0.5 nm.

3. Experimental findings and their discussion

PCL spectra of Nd^{3+}:YAG monocrystals and ceramics have the same structure of bands (Fig. 1, a). In the ultraviolet (UV) and visible (VD) ranges of the spectrum the bands of optical transitions from the $^2F2_{5/2}$ level with electron configuration $4f^25d^1$, split into three Stark components ($\nu_0 = 37775$, $\nu_1 = 37864$ and $\nu_2 = 38153\,cm^{-1}$ [5,6]), to the levels of the neodymium ion $4f^3$ configuration are observed. In the near infrared (IR) region an intracenter $f-f$ luminescence of the neodymium ion is observed at transitions from the $^4F_{3/2}$ level to $^4I_{9/2}$ and $^4I_{11/2}$ levels [10].

The PCL spectra of ceramics and nanopowders based on neodymium activated yttrium oxide are also similar to each other (Fig. 1, b). Note that luminescence from the $^2F2_{5/2}$ level was not observed in this crystal matrix, but only $f-f$-transitions in the IR region were observed, where two groups of bands from the $^4F_{5/2}$ and $^4F_{3/2}$ luminescent levels to $^4I_{9/2}$ and $^4I_{11/2}$ levels are distinguished.
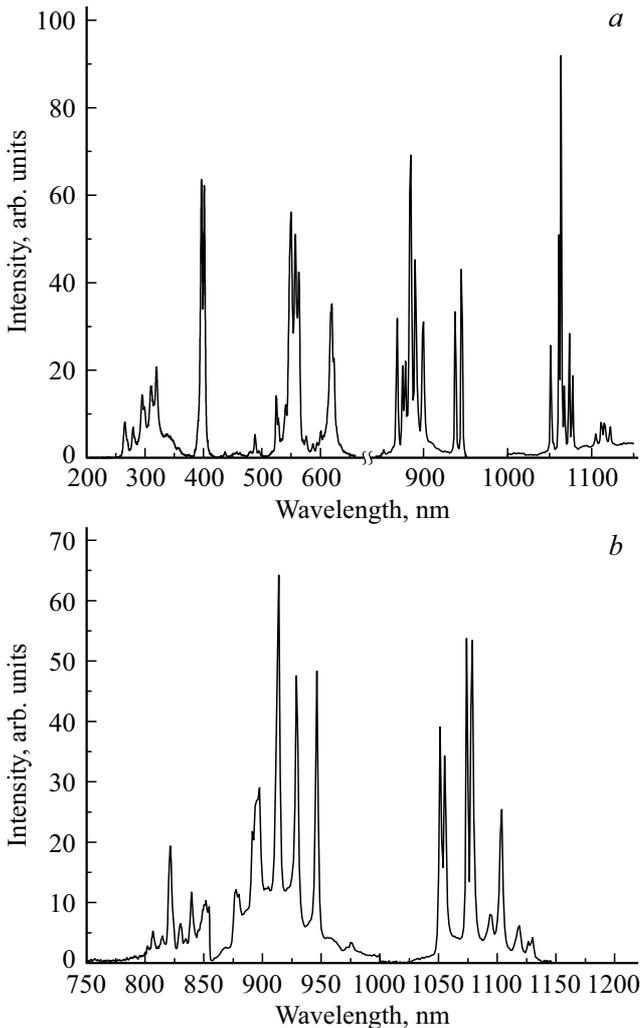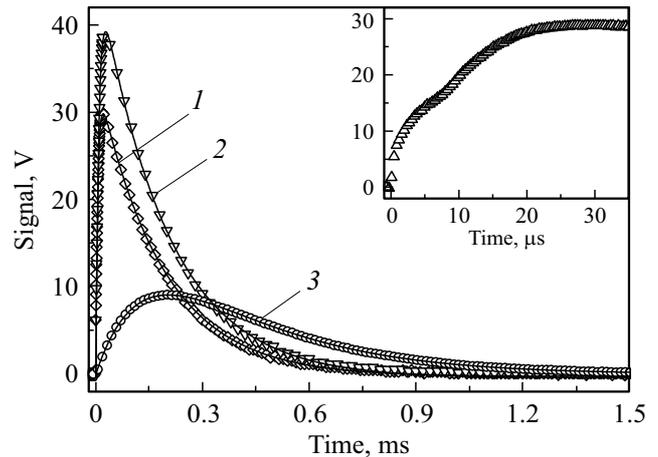

Figure 2. Typical luminescence kinetics of Nd^{3+}:YAG spectral bands located in: 1 — UV ($\lambda = 321\,nm$), 2 — VD ($\lambda = 461\,nm$), and 3 — IR ($\lambda = 1052\,nm$) regions. The inset shows the typical area of the band rise at $\lambda = 396\,nm$.

Figure 1. Pulsed cathodoluminescence spectra of single crystal Nd^{3+}:YAG (a) and ceramic sample Nd^{3+}:Y_2O_3 (b).

The most important information about the luminescence centers is contained in the luminescence kinetics [11]. The characteristic curves of the bands kinetics for three spectral regions of Nd^{3+}:YAG are shown in Fig. 2. The pattern of the kinetics of band intensity for ceramics and nanopowders of the system based on yttrium oxide is similar to the curve 3 in Fig. 2. The kinetics of all neodymium bands is characterized by the presence of a maximum, and the times of its reaching for the bands of the ultraviolet (curve 1) and visible (curve 2) regions of Nd^{3+} in YAG are close and equal to 21 and 27 μs respectively, while for the infrared region of YAG and Y_2O_3 (curve 3) this time is by an order of magnitude longer and is on the average about 200 μs.

For the sake of argument, let us call the temporal behavior of the intensities before the maximum is reached by the rise, and after the maximum — by the decay of the luminescence. For each luminescence band corresponding to the optical transition from the luminescent level i to the below located level k, the kinetic curve $I_{ik}(t)$ is described by a regression line with a coefficient $r^2 = 0.99$ (in Fig. 2, solid lines) as the difference of two exponential functions

$$I_{ik}(t) = I_{0ik}(t)\left[\exp\left(-\frac{t}{\tau_2}\right) - \exp\left(-\frac{t}{\tau_1}\right)\right]. \quad (1)$$

In this formula $I_{0ik}(t)$ is the intensity at the maximum, t is current time, $\tau_1 < \tau_2$ are the time constants of the luminescence rise and decay processes.

To clarify the nature of these processes, let us consider the kinetic equation describing the temporal behavior of the luminescence intensity of the spectral band at λ_{ik} of the luminescence center (LC), which is proportional to the population C_i of its luminescent level. After switching off the electron beam, the population of the i-th luminescent level will be determined by the kinetic equation

$$\frac{dC_i}{dt} = f(t) - \frac{C_i}{\tau_i}, \quad (2)$$

where τ_i is the effective lifetime of the luminescent level, $f(t)$ is a function that takes into account this level pumping in the processes of recombination of electron-hole pairs created in the sample by electrons of the beam with a concentration of nonequilibrium charge carriers n_e and the processes of energy transfer from the upper excited levels of LC with the population C_j ($j > i$).

After the excitation switching off, the concentration of nonequilibrium charge carriers decreases in accordance with the kinetic equation

$$\frac{dn_e}{dt} = -Bn_e^2 - An_e, \qquad (3)$$

where B is the rate constant of the formation of free and self-trapped excitons, $A = kN^+$ is the probability of capture of a free electron by localized holes whose concentration is equal to N^+, k is the rate constant of this capture and is of the order of $10^{-10}\,\text{cm}^3/\text{s}$ (linear recombination). In this case, the pumping function for the level, above which there are no excited states, takes the form

$$f(t) = \beta_i Bn_e^2 + \alpha_i An_e, \qquad (4)$$

where β_i and α_i are the branching coefficients that determine the fraction of recombination processes leading to the excitation of precisely i-th LC level.

For the solution of equation (2) to have the form of the experimentally observed relationship (1), the pumping function $f(t)$ should be exponential. This situation arises when the dominant pumping mechanism is the linear recombination of electron-hole pairs, where a free electron e is captured by the ionized luminescence center C^+, and the luminescence center C_i excited to i-th level is formed

$$e + C^+ \rightarrow C_i + \Delta E \qquad (5)$$

with the release of excess energy ΔE, for example, in the form of phonon generation. Then, in formulas (3) and (4), the first term in the right-hand side can be neglected, and the expression for the pumping function and the kinetic equation for the population of the C_i level take the form

$$f(t) = \alpha_i An_e, \qquad (6a)$$

$$\frac{dC_i}{dt} = \alpha_i \frac{n_{e0}}{\tau_r} \exp\left(-\frac{t}{\tau_r}\right) - \frac{C_i}{\tau_i}. \qquad (6b)$$

Here $\tau_r = A^{-1} = (kC^+)^{-1}$ is the characteristic time of linear recombination in reaction (5), n_{e0} is the concentration of free electrons created by the beam electrons towards the end of the pulse.

With an electron beam duration of 2 ns, we are dealing with an „instantaneous" excitation pulse, during the action of which luminescence does not have time to develop. Therefore, $C_i(t = 0) = 0$ should be taken as the initial condition of equation (6b), and then the solution becomes

$$C_i = \alpha_i \frac{n_{e0}\tau_i}{\tau_i - \tau_r}\left[\exp\left(-\frac{t}{\tau_i}\right) - \exp\left(-\frac{t}{\tau_r}\right)\right], \qquad (7)$$

qualitatively matching with the experimental curve (*1*).

In the presence of excited states of LC j, located above the luminescence level i, it is additionally pumped by energy transfer from the j levels. In this case, additional terms should be included in the excitation function $f(t)$ (6a)

$$f(t) = \alpha_i An_e + \sum_{j > i} \frac{C_j}{\tau_{ji}}, \qquad (8)$$

in which the populations C_j are described by formulas similar to (7), τ_{ji} is the characteristic time of energy transfer from the j level to i level by radiative and nonradiative paths. This pumping leads, first of all, to a time delay of the luminescence rise and, secondly, to a change in the luminescence decay law. Namely, for $\tau_{ji} > \tau_i$ the decay of the intensity is determined by the sum of exponentials with the characteristic times τ_{ji} and τ_i, and in the remote afterglow — with the characteristic time equal to the greater of τ_{ji} and τ_i.

Note that the luminescence rise effect is well known for phosphors [12]. In them, the stage of rise appears as luminescence intensity increasing to stationary value during the excitation action, i.e. due to ionization and excitation processes. In our case, the luminescence rise is observed after the excitation due to recombination and relaxation processes. This fact should be paid attention when measuring the characteristic lifetimes of the luminescent levels under the conditions of stationary cathodoluminescence [7] and electron beam with long duration [13], for which the absolute intensity maximum is reached by the end of the electron beam. Under these conditions, at the moment of switching off the electron beam, the population of the luminescent level is $C_i(t = 0) = C_{i0} > 0$, which is the initial condition of equation (6b). Then solution (6b) takes the form

$$C_i = \alpha_i \frac{n_{e0}\tau_i}{\tau_i - \tau_r}\left[\exp\left(-\frac{t}{\tau_i}\right) - \exp\left(-\frac{t}{\tau_r}\right)\right] + C_{i0}\exp\left(-\frac{t}{\tau_i}\right). \qquad (9)$$

The graph of function (9) is a nonmonotonically decrement curve with a local maximum or inflection caused by additional population of the luminescent level in recombination and relaxation processes. At $\tau_i > \tau_r$, the intensity decreasing in the near afterglow is determined by the characteristic time τ_r, and in the remote afterglow — τ_i. The picture does not change qualitatively when the additional population of the luminescent level by other mechanisms (8) is taken into account. Accordingly, neglecting the additional population leads to to an erroneous interpretation of the kinetic data.

Correct approximation of the obtained experimental relationships by expression (1) made it possible to determine the kinetic parameters τ_1 and τ_2 for the observed bands in the samples under study. Note that measurements carried out at different values of the average energy of electrons (130, 150 and 170 keV) did not reveal any features or differences in the kinetic parameters. Therefore, all the given below characteristic luminescence rise and decay

Characteristic times τ_1 and τ_2 of spectral bands of the system $Nd^{3+}:YAG$ and $Nd^{3+}:Y_2O_3$

$Nd^{3+}:YAG$				
Luminescent level (Stark component)	τ_1, μs		τ_2, μs	
	crystal	ceramics	crystal	ceramics
$^2F2_{5/2}$ (ν_2)	4.5 ± 0.2		175.0 ± 2.0	190.0 ± 3.0
$^2F2_{5/2}$ (ν_1)	7.0 ± 0.2		180.0 ± 3.0	192.0 ± 3.0
$^2F2_{5/2}$ (ν_0)	12.0 ± 0.9		195.0 ± 4.0	210.0 ± 2.0
$^4F_{3/2}$	135.0 ± 5.0	95.0 ± 3.0	290.0 ± 2.0	

$Nd^{3+}:Y_2O_3$				
Luminescent level	τ_1, μs		τ_2, μs	
	nanopowder	ceramic	nanopowder	ceramic
$^4F_{5/2}$	90.0 ± 6.0	112.0 ± 13.0	530.0 ± 18.0	308.0 ± 60.0
$^4F_{3/2}$	91.0 ± 2.0	95.0 ± 8.0	533.0 ± 9.0	331.0 ± 18.0

times correspond to measurements at an average energy of electrons of 150 keV.

In all $Nd^{3+}:YAG$ samples the observed luminescence lines of neodymium ions are clearly divided into 4 groups. The luminescent levels of the first three groups of spectral bands are the three Stark components of the level $^2F2_{5/2}$ of the neodymium ion with the electron configuration $4f^2 5d^1$. Of these, the most numerous group of bands is observed from the upper Stark level with $\nu_2 = 38153\,cm^{-1}$ ($\lambda = 265.6, 270.0, 280.0, 283.0, 295.5, 300.6, 310.8, 321.0, 413.0, 429.5, 450.0, 456.0, 461.0, 480.0, 487.5, 494.5, 540.5, 576.5, 586.5, 596.0, 601.0$ and $619.0\,nm$). For the second group of bands ($\lambda = 435.0, 525.0, 549.0, 556.0$ and $560.5\,nm$), the middle Stark level with $\nu_1 = 37864\,cm^{-1}$ is luminescent level. For the third group of bands ($\lambda = 396.0$ and $400.5\,nm$), the lower Stark level with $\nu_0 = 37775\,cm^{-1}$ is luminescent level. For the fourth group of near IR bands ($\lambda = 869.0, 885.0, 891.0, 900.0, 938.0, 946.0, 1052.0, 1064.0, 1074.0, 1104.0, 1111.0, 1115.0$ and $1120.0\,nm$), there is the $^4F_{3/2}$ luminescent level of Nd^{3+} ion with the electron configuration $4f^3$. Note that there are no luminescent transitions to it from the level $^2F2_{5/2}$. The Table lists the characteristic times τ_1 and τ_2 for the spectral bands from the corresponding luminescent levels.

In the $Nd^{3+}:YAG$ system, the level $^2F2_{5/2}$ is the highest luminescent level, which, as above mentioned, is split into three Stark sublevels. The topmost sublevel ν_2 has no additional pumping sources. The measured rise time of spectral bands for which this sublevel is luminescent is $\tau_1 = \tau_r = (kC^+)^{-1} = 4.5\,\mu s$. This means that the concentration of luminescence centers ionized by the electron beam is of the order of $10^{16}\,cm^{-3}$, which is much less than the concentration of impurity neodymium ions (aboud $10^{20}\,cm^{-3}$). Two other Stark sublevels (ν_1 and ν_0) of the $^2F2_{5/2}$ level are additionally pumped due

to nonradiative transitions from the upper components. These sources lead to the appearance of an inflection in the rise curves (inset in Fig. 2) of the luminescence bands starting from the sublevels ν_1 and ν_0, as a result of which the rise time increases to 7 and $12\,\mu s$, respectively. With the number of pumping channels increasing the rise curves again become smooth and are well described by an exponential law. This is already observed for the bands from the lowest sublevel ν_0 in the $^2F2_{5/2}$ system, and is especially evident for the spectral bands starting from the $^4F_{3/2}$ luminescent level of Nd^{3+} ion. For the latter, the rise time is by order of magnitude longer than that of the bands from the $^2F2_{5/2}$ luminescent level. Moreover, the spectrum does not include the bands of optical transitions $^2F2_{5/2} \rightarrow ^4F_{3/2}$, i.e. the main pumping mechanism of level $^4F_{3/2}$ is Nonradiative transitions from the upper levels. The decay time τ_2 for all bands from this level is $290\,\mu s$ (Table) in ceramic and monocrystal samples. This value is in good agreement with the lifetime of the $^4F_{3/2}$ level measured upon photoexcitation ($230\,\mu s$) [1]. These bands are characterized by a strong difference in the rise time τ_1 for single crystals ($135\,\mu s$) and ceramic samples ($95\,\mu s$), which is associated with the presence in the ceramics of a competing transmission channel from the upper levels of neodymium ion $4f^3$ configuration, for example, energy transfer to structural centers formed by ions of sintering additives. This effect is also evident in the intensity decreasing of all IR-bands in ceramics as compared to single crystals.

In $Nd^{3+}:Y_2O_3$ nanopowder and ceramic samples luminescence is observed from levels $^4F_{5/2}$ (821.6, 830.1, 839.6, 851.8), $^4F_{3/2}$ (878.0, 880.0, 894.0, 897.5, 914.0, 929.0, 946.3) levels to $^4I_{9/2}$ and from $^4F_{3/2}$ level to $^4I_{11/2}$ (1051.3, 1055.0, 1073.8, 1078.8, 1094.0, 1103.8). For the said spectral bands of the neodymium ion in the yttrium

oxide system the kinetic characteristics are also summarized in the Table. The $^4F_{3/2}$ and $^4F_{5/2}$ luminescent levels are strongly coupled, which is indicated by the close values of the rise and decay times of luminescence from these levels in different samples. These levels, as in the Nd : YAG system, are populated due to cascade transitions from the upper levels of the neodymium ion. However, the mechanism of populating the upper levels is not clear, since the $^2F2_{5/2}$ level of the neodymium ion dois not does not appear in luminescence. Note also the shorter lifetime τ_2 in ceramic samples as compared to nanoparticles, which may be due to the presence of a larger number of structural defects in ceramics. Besides, note also the greater scatter in the values of the times τ_1 and τ_2 in Nd : Y_2O_3, as compared with Nd : YAG, which is most likely due to the presence in yttrium oxide system of uncontrolled impurities capable of depopulating the luminescent levels.

4. Conclusion

Thus, the kinetics of pulsed cathodoluminescence of all neodymium bands in yttrium-aluminum garnet and in yttrium oxide is characterized by the rise and decay described by the difference of two exponential functions. The characteristic decay time of luminescence for these materials does not depend on the electron energy and is the lifetime of the luminescent level, and the rise time is determined by the mechanism of its pumping. At a short duration of the exciting electron beam (2 ns) the pumping of the luminescent level occurs in the process of recombination of electron-hole pairs created in the substance by the electrons of the exciting beam, and due to the relaxation of the excitation energy of the upper levels. So, for pulse cathodoluminescence the recombination-relaxation mechanism of pumping of the luminescent levels is characteristic, which differs significantly from „phosphors ignition", occurred during ionization and excitation of the phosphor by an external source.

Conflict of interest

The authors declare that they have no conflict of interest.

References

[1] A.M. Prokhorov. Spravochnik po lazeram / Ed. A.M. Prokhorov. Sov. radio, M. (1978). V. 1. 504 p. (in Russian)
[2] A. Ikesue, T. Kinoshita, K. Kamata, K. Yoshida. Am. Ceram. Soc. **78**, *4*, 1033 (1995).
[3] J. Lu, M. Prabhu, J. Xu., K. Ueda, H. Yagi, T. Yanagitani, A. Kaminskii. Jpn. J. Appl. Phys. **39**, *10B*, 1048 (2000).
[4] S.N. Bagayev, V.V. Osipov, V.I. Solomonov, V.A. Shitov, R.N. Maksimov, K.E. Lukyashin, S.M. Vatnik, I.A. Vedin. Opt. Mater. **34**, *8*, 1482 (2012).
[5] A.I. Kolomijtsev, M.L. Mejl'man, I.S. Volodina, M.V. Chukichev, A.G. Smagin, Kh.S. Bagdasarov. Optika i spektroskopiya **56**, *2*, 365 (1984). (in Russian)
[6] V.V. Osipov, V.I. Solomonov, A.V. Spirina. Opt. zhurn. **78**, *6*, 81 (2011). (in Russian)
[7] K.N. Gulyaeva, A.N. Trofimov, M.V. Zamoryanskaya. **114**, *5*, 773 (2013). (in Russian)
[8] K.K. Deb, R.G. Buser, J. Paul. Appl. Opt. **20**, *7*, 1203 (1981).
[9] V. Lupei, A. Lupei, C. Tiseanu, S. Georgescu, C. Stoicescu, P.M. Nanau. Phys. Rev. B **51**, *1*, 8 (1995).
[10] A.A. Kaminsky. Lazernye kristally. Nauka, M. (1975). 256 p. (in Russian)
[11] V.I. Solomonov. Optika i spektroskopiya **95**, *2*, 266 (2003). (in Russian)
[12] O.N. Kazgikin, L.Ya. Markovsky, I.A. Mironov, F.M. Pskerman, L.N. Petoshina. Neorganicheskie lyuminofory. Khimiya, M. (1975). 192 p. (in Russian)
[13] E.I. Lipatov, V.M. Lisitsyn, V.I. Oleshko, V.F. Tarasenko. Izv. vuzov. Fizika **50**, *1*, 53 (2007). (in Russian)

The publication of seminar papers will be continued in Physics of the Solid State, No.12/21